

**Three-dimensional rogue waves in nonstationary parabolic potentials**Zhenya Yan,<sup>1,2,\*</sup> V. V. Konotop,<sup>3</sup> and N. Akhmediev<sup>4</sup><sup>1</sup>*Key Laboratory of Mathematics Mechanization, Institute of Systems Science, AMSS, Chinese Academy of Sciences, Beijing 100080, China*<sup>2</sup>*International Centre for Materials Physics, Chinese Academy of Sciences, Shenyang 110016, China*<sup>3</sup>*Centro de Física Teórica e Computacional and Departamento de Física, Faculdade de Ciências, Universidade de Lisboa, Lisboa 1649-003, Portugal*<sup>4</sup>*Optical Sciences Group, Research School of Physics and Engineering, Institute of Advanced Studies, The Australian National University, Canberra, Australian Capital Territory 0200, Australia*

(Received 1 August 2010; published 30 September 2010)

Using symmetry analysis we systematically present a higher-dimensional similarity transformation reducing the (3+1)-dimensional inhomogeneous nonlinear Schrödinger (NLS) equation with variable coefficients and parabolic potential to the (1+1)-dimensional NLS equation with constant coefficients. This transformation allows us to relate certain class of localized exact solutions of the (3+1)-dimensional case to the variety of solutions of integrable NLS equation of the (1+1)-dimensional case. As an example, we illustrated our technique using two lowest-order rational solutions of the NLS equation as seeding functions to obtain rogue wavelike solutions localized in three dimensions that have complicated evolution in time including interactions between two time-dependent rogue wave solutions. The obtained three-dimensional rogue wavelike solutions may raise the possibility of relative experiments and potential applications in nonlinear optics and Bose-Einstein condensates.

DOI: [10.1103/PhysRevE.82.036610](https://doi.org/10.1103/PhysRevE.82.036610)

PACS number(s): 05.45.Yv, 42.65.Tg, 42.50.Gy, 03.75.Lm

**I. INTRODUCTION**

Similarity analysis is one of the modern powerful techniques which allows us to find self-similar solutions of equations that previously were known to be nonintegrable (see, e.g., [1] and references therein). They do not provide the complete integrability. However, they help to produce selected solutions in analytical form, which may be important for a variety of applications. One of the representative examples is the nonlinear Schrödinger (NLS) equation. It is well known that in (1+1)-dimensions [(1+1)-D] this equation is completely integrable by inverse scattering technique [2]. In (2+1)-D the equation is not integrable. However, solutions localized in two transverse directions do exist [3], but may be unstable and subjected to collapse [4,5]. They are mostly known from numerical simulations [6]. Remarkably, some of the localized solutions can be found using similarity reductions [7]. Despite being unphysical, exact solutions provide some insight on the properties of the equation that is important for many applications. Clearly, adding a dimension changes drastically integrability properties of the equation. Thus, the (3+1)-dimensional NLS equation is not an exception, and we are faced with the problem of finding its solutions knowing that they are not directly related to the solutions of the same equation in lower dimensionality.

The NLS equation in (3+1)-D is an important model for a variety of physical problems [8,9]. It is used in nonlinear optics [8], condensed-matter physics, and in particular in modeling Bose-Einstein condensate (BEC) [9]. Numerical solutions can be found with various techniques, but the value of an analytical approach is significant by itself. In this work,

extending the ideas of [10,11] we use the similarity transformations to reduce the dimensionality of the equation from (3+1)-D to (1+1)-D. In the former case, the coefficients in the equation are variable, while in the latter they can be chosen to be constants. This allows us to use the complete integrability of the (1+1)-dimensional equation.

More specifically, we will focus on the possibility of constructing truly three-dimensional (3D) rogue waves, i.e., waves whose dynamics essentially depends on all spatial coordinates, although it is possible to identify the coordinate in which the motion is effectively one dimensional. This example is directly related to the description of matter wave dynamics in the mean-field approximation (where the NLS equation is also known as the Gross-Pitaevskii equation), thus representing a unique possibility of creating and observing three-dimensional rogue matter waves. We note that the conventional rogue waves are either two dimensional, as it happens, e.g., in the ocean [12], in wide aperture optical cavities [13], and in capillary wave experiments [14], or one dimensional and they appear in many fields including nonlinear optics [15–18], cigar-shaped BECs [19], atmosphere [20], and finances [21].

The rest of this paper is organized as follows. In Sec. II, we describe the (1+1)-dimensional similarity transformation reducing the (3+1)-dimensional inhomogeneous NLS equation with variable coefficients and parabolic potential to the (1+1)-dimensional NLS equation with constant coefficients. In Sec. III, we determine the self-similar variables and constraints satisfied by the coefficients in the (3+1)-dimensional inhomogeneous NLS equation. Moreover, we give some comments about these coefficients. Section IV mainly discusses two types of localized 3D rogue wavelike solutions, which profiles are exhibited. Finally, we give some conclusions in Sec. V.

\*zyyan\_math@yahoo.com

## II. 3D MODEL AND SIMILARITY REDUCTIONS

The original three-dimensional inhomogeneous NLS equation with variable coefficients can be written in a dimensionless form,

$$i\frac{\partial\Psi}{\partial t} = -\frac{1}{2}\nabla^2\Psi + v(\mathbf{r},t)\Psi + g(t)|\Psi|^2\Psi + i\gamma(t)\Psi, \quad (1)$$

where the physical field  $\Psi \equiv \Psi(\mathbf{r}, t)$ ,  $\mathbf{r} \in \mathbb{R}^3$ ,  $\nabla \equiv (\partial_x, \partial_y, \partial_z)$  with  $\partial_x \equiv \partial/\partial x$ , the external potential  $v(\mathbf{r}, t)$  is a real-valued function of time and spatial coordinates, and the nonlinear coefficient  $g(t)$  and gain or loss coefficient  $\gamma(t)$  are real-valued functions of time. This equation arises in many fields such as nonlinear optics (see, e.g., [8]) and BECs (also known as the three-dimensional Gross-Pitaevskii equation with variable coefficients; see, e.g., [9–11]).

We search for a similar transformation connecting solutions of Eq. (1) with those of the (1+1)-dimensional standard NLS equation with constant coefficients, i.e.,

$$i\frac{\partial\Phi(\eta, \tau)}{\partial\tau} = -\frac{\partial^2\Phi(\eta, \tau)}{\partial\eta^2} + G|\Phi(\eta, \tau)|^2\Phi(\eta, \tau). \quad (2)$$

Here, the physical field  $\Phi(\eta, \tau)$  is a function of two variables  $\eta \equiv \eta(\mathbf{r}, t)$  and  $\tau \equiv \tau(t)$ , which are to be determined, and  $G$  is a constant. Since our main goal is to study three-dimensional rogue waves, we choose  $G=-1$  which corresponds to the attractive case (or focusing nonlinearity in optics and negative scattering lengths in the BEC theory). In order to control boundary conditions at infinity we impose the natural constraints [10]

$$\eta \rightarrow 0 \quad \text{at } \mathbf{r} \rightarrow 0, \quad \eta \rightarrow \infty \quad \text{at } \mathbf{r} \rightarrow \infty. \quad (3)$$

We are looking for the physical field  $\Psi(\mathbf{r}, t)$  in the form of the ansatz [11]

$$\Psi(\mathbf{r}, t) = \rho(t)e^{i\varphi(\mathbf{r}, t)}\Phi[\eta(\mathbf{r}, t), \tau(t)], \quad (4)$$

with  $\rho(t)$  and  $\varphi(\mathbf{r}, t)$  [like  $\tau(t)$  and  $\eta(\mathbf{r}, t)$ , introduced above] being the real-valued functions of the indicated variables. Ansatz (4) allows us to reduce the problem to the (1+1)-dimensional one (we notice that it differs from the one-dimensional stationary reductions [10,22]). Variables in this reduction are to be determined from the requirement for the new function  $\Phi(\eta(\mathbf{r}, t), \tau(t))$  to satisfy Eq. (2) [we notice that there also exist other similar reductions for Eq. (1) which require that  $\Phi(\eta, \tau)$  may satisfy other nonlinear equations]. Thus, we substitute transformation (4) into Eq. (1) and after relatively simple algebra obtain the system of partial differential equations

$$\nabla^2\eta = 0, \quad \eta_t + \nabla\varphi \cdot \nabla\eta = 0, \quad 2\tau_t - |\nabla\eta|^2 = 0, \quad (5a)$$

$$2\rho_t + \rho\nabla^2\varphi - 2\gamma(t)\rho = 0, \quad (5b)$$

$$2g(t)\rho^2 - G|\nabla\eta|^2 = 0, \quad (5c)$$

$$2v(\mathbf{r}, t) + |\nabla\varphi|^2 + 2\varphi_t = 0. \quad (5d)$$

Generally speaking, equations in system (5) are not compatible with each other when linear and nonlinear potentials

are arbitrary. One, however, can pose the problem to find the functions  $v(\mathbf{r}, t)$ ,  $g(t)$ , and  $\gamma(t)$  such that system (5) becomes solvable. This requirement leads us to the procedure which can be outlined as follows:

(i) First, we solve Eq. (5a) subject to the boundary conditions (3), thus obtaining the similarity variables  $\eta(\mathbf{r}, t)$ ,  $\tau(t)$ , and the phase  $\varphi(\mathbf{r}, t)$ .

(ii) Second, we consider Eqs. (5b)–(5d) as definitions for the functions  $\rho(t)$ ,  $v(\mathbf{r}, t)$ , and  $g(t)$  in terms of already known functions  $\eta(\mathbf{r}, t)$ ,  $\tau(t)$ , and  $\varphi(\mathbf{r}, t)$ .

Note that the first step determines transformation of variables which does not involve explicitly any specific time-dependent coefficients. However, these coefficients may appear after integration of these equations. The second step determines the coefficients which are compatible with the above change of variables. Thus, it leads to model (2). In this approach, the function  $\eta(\mathbf{r}, t)$  defines the surface where the wave has a constant amplitude. The function  $\varphi(\mathbf{r}, t)$  determines the wave-front solution (the manifold of the constant phase).

Thus, we can establish a correspondence between selected solutions of the (3+1)-dimensional inhomogeneous NLS equation with variable coefficients (1) and known solutions of completely integrable NLS equation (2). The latter has an infinite number of solutions, thereby giving us a chance to look for physically relevant solutions of the (3+1)-dimensional case. In particular, we can relate them to the recently studied rogue wave solutions of the NLS equation [23–26]. As a consequence, we obtain three-dimensional time-dependant rogue wave solutions of Eq. (1).

## III. VARIABLES AND COEFFICIENTS OF THE TRANSFORMATION

Solving Eq. (5a) we can write the similarity variables  $\eta(\mathbf{r}, t)$ ,  $\tau(t)$ , and the phase  $\varphi(\mathbf{r}, t)$  in the form

$$\eta(\mathbf{r}, t) = \mathbf{c}(t) \cdot \mathbf{r} - \int_0^t \mathbf{c}(s) \cdot \mathbf{a}(s) ds, \quad (6a)$$

$$\tau(t) = \frac{1}{2} \int_0^t |\mathbf{c}(s)|^2 ds, \quad (6b)$$

$$\varphi(\mathbf{r}, t) = \mathbf{r}\hat{\Omega}(t)\mathbf{r} + \mathbf{a}(t) \cdot \mathbf{r} + \omega(t), \quad (6c)$$

where we have introduced the diagonal time-dependent  $3 \times 3$  matrix  $\hat{\Omega}(t) = \text{diag}[\Omega_x(t), \Omega_y(t), \Omega_z(t)]$  with  $\Omega_\sigma(t) = -\dot{c}_\sigma(t)/[2c_\sigma(t)]$  (hereafter,  $\sigma=x, y, z$  and an overdot stands for the derivative with respect to time). The coefficients  $\mathbf{c}(t) = [c_x(t), c_y(t), c_z(t)]$ ,  $\mathbf{a}(t) = [a_x(t), a_y(t), a_z(t)]$ , and  $\omega(t)$  are time-dependent functions. Now, from Eqs. (5b)–(5d) we obtain the functions  $\rho(t)$ ,  $v(\mathbf{r}, t)$ , and  $g(t)$  in the form

$$\rho(t) = \rho_0 \sqrt{|c_x(t)c_y(t)c_z(t)|} \exp \left[ \int_0^t \gamma(s) ds \right], \quad (7a)$$

$$g(t) = \frac{G|\mathbf{c}(t)|^2}{2\rho_0^2 |c_x(t)c_y(t)c_z(t)| \exp \left[ 2 \int_0^t \gamma(s) ds \right]}, \quad (7b)$$

$$v(\mathbf{r}, t) = \mathbf{r} \hat{A}(t) \mathbf{r} + \mathbf{b}(t) \cdot \mathbf{r} - \dot{\omega}(t) - \frac{1}{2} |\mathbf{a}(t)|^2, \quad (7c)$$

where  $\rho_0$  is an integration constant.

A few comments would be useful here. First, the gain or loss term  $\gamma(t)$  is determined in the initial statement of the problem and can serve as an additional control function or a parameter if it is a constant. Then changing the time-dependent dissipation, we can excite different dynamical regimes. Second, the change of the all parameters is interrelated. In practical terms such a time dependence can be performed in different ways for different physical systems. In particular, in the context of the BEC applications, this can be done by simultaneous change of the frequency of the lasers controlling the external trap  $v(\mathbf{r}, t)$  and the detuning from the Feshbach resonance, responsible for the variation of  $g(t)$ . Finally, we notice that one can consider the case of  $g(t) \equiv \text{const}$ , which however is reduced to the trivial case of a plane wave, whose parameters change along the chosen direction (determined by the vector  $\mathbf{c}$  which is a constant in this case). Such solutions will not be considered here.

In writing the linear potential  $v(\mathbf{r}, t)$  we have defined the diagonal time-dependent  $3 \times 3$  matrix  $\hat{A}(t) = \text{diag}[A_x(t), A_y(t), A_z(t)]$  with the entries

$$A_\sigma(t) = \frac{\ddot{c}_\sigma(t)}{2c_\sigma(t)} - \frac{\dot{c}_\sigma^2(t)}{c_\sigma^2(t)}, \quad (8)$$

and the vector function  $\mathbf{b}(t) = [b_x(t), b_y(t), b_z(t)]$  with the entries

$$b_\sigma(t) = \frac{\dot{c}_\sigma(t) a_\sigma(t)}{c_\sigma(t)} - \dot{a}_\sigma(t). \quad (9)$$

It is easy to see that the velocity field  $\mathbf{v}(\mathbf{r}, t) = \nabla \varphi(\mathbf{r}, t)$  corresponding to the above-mentioned phase  $\varphi(\mathbf{r}, t)$  is given by

$$\mathbf{v}(\mathbf{r}, t) = 2[\Omega_x(t)x, \Omega_y(t)y, \Omega_z(t)z] + \mathbf{a}(t), \quad (10)$$

such that we have the divergence of the vector field  $\mathbf{v}(\mathbf{r}, t)$  in the form

$$\text{div } \mathbf{v}(\mathbf{r}, t) = 2[\Omega_x(t) + \Omega_y(t) + \Omega_z(t)] = -\partial_t \ln |c_x(t)c_y(t)c_z(t)|. \quad (11)$$

Thus, the zeros of any of the components of  $\mathbf{c}(t)$  mean the divergence of the field, which occurs at the instants when the nonlinearity  $g(t)$  becomes infinite [see Eq. (7b)]. Such cases will not be considered in the present paper.

It follows from Eqs. (7c) and (8) that if we require that the linear potential  $v(\mathbf{r}, t)$  is a second degree polynomial for every space  $x, y, z$ , then we have  $A_\sigma \neq 0$ , i.e.,  $c_\sigma \ddot{c}_\sigma - 2\dot{c}_\sigma^2 \neq 0$ , which denotes that  $c_\sigma$ 's are not equivalent to constants, but are some functions of time. These time-dependent functions  $c_\sigma(t)$  will affect the other variables [see Eqs. (6a)–(6c), (7a)–(7c), (8), and (9)] such that self-similar solutions of Eq. (1) in form (4) exhibit abundant structures. In what follows we will use specific solutions (e.g., rogue wave solutions) of the NLS equation to illustrate the nontrivial dynamics of three-dimensional rogue wavelike solutions defined by Eq. (1) for the different parameters mentioned above.

#### IV. TWO TYPES OF LOCALIZED 3D ROGUE WAVELIKE SOLUTIONS

As two representative examples, we consider the lowest-order rational solutions of the NLS equation which serve as prototypes of rogue waves. First, we use the first-order rational solution of Eq. (2) (see [23]). As a result, we obtain the first-order nonstationary rogue wave solutions of Eq. (1) in the form

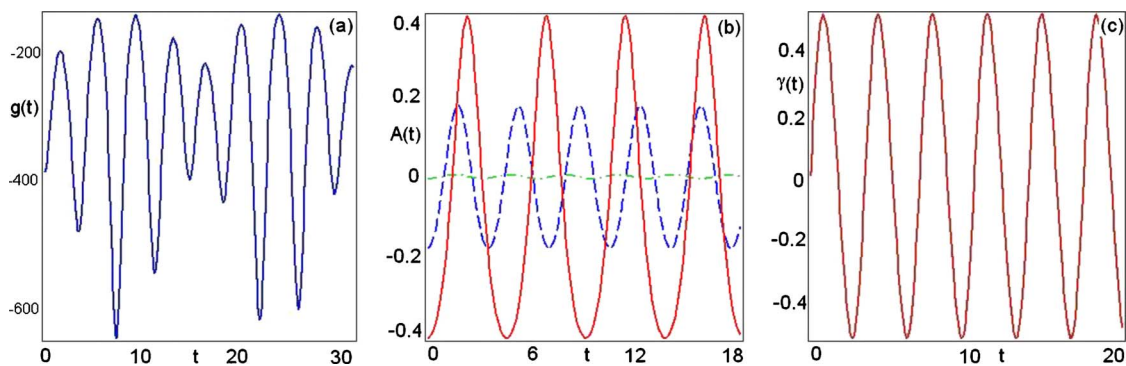


FIG. 1. (Color online) Profiles of (a) nonlinearity  $g(t)$  given by Eq. (7b); (b) the coefficients  $A_x(t)$  (solid line),  $A_y(t)$  (dashed line), and  $A_z(t)$  (dashed-dotted line) of second degree term of the linear potential  $v(\mathbf{r}, t)$  given by Eq. (8); and (c) the gain or loss term  $\gamma(t)$  vs time for the parameters are given by Eq. (13) with  $k_x=0.9$ ,  $k_y=0.6$ ,  $k_z=0.1$ , and  $k=0.6$ .

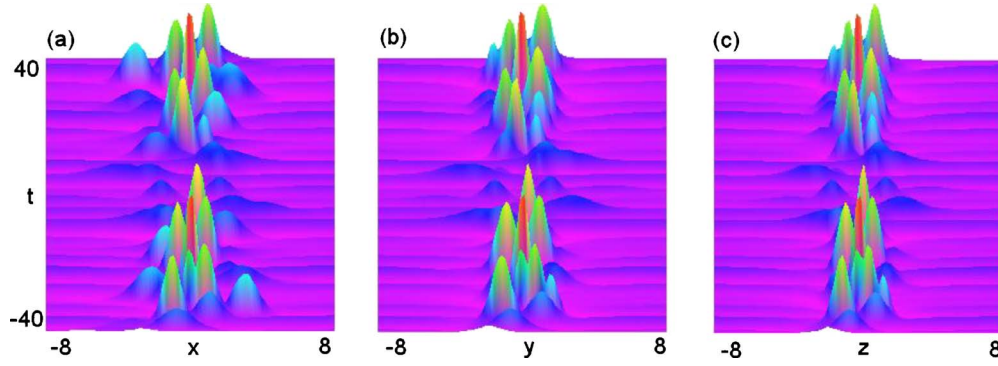


FIG. 2. (Color online) Color coded plot of wave intensity (a)  $|\Psi_1|^2(x,0,0,t)$  with  $\max_{\{x,0,0,t\}}|\Psi_1|^2=0.06$ , (b)  $|\Psi_1|^2(0,y,0,t)$  with  $\max_{\{0,y,0,t\}}|\Psi_1|^2=0.068$ , and (c)  $|\Psi_1|^2(0,0,z,t)$  with  $\max_{\{0,0,z,t\}}|\Psi_1|^2=0.068$  defined by solution (12) for the parameters given by Eq. (13) with  $k_x=0.9$ ,  $k_y=0.6$ ,  $k_z=0.1$ ,  $k=0.6$ . Note that for a given set of parameters, the wave is localized in space.

$$\Psi_1(\mathbf{r},t) = \rho_0 \sqrt{|c_x(t)c_y(t)c_z(t)|} \exp \left[ \int_0^t \gamma(s) ds \right] \times \left[ 1 - \frac{4 + 8i\tau(t)}{1 + 2\eta^2(\mathbf{r},t) + 4\tau^2(t)} \right] e^{i[\varphi(\mathbf{r},t) + \tau(t)]}, \quad (12)$$

where the variables  $\eta(\mathbf{r},t)$ ,  $\tau(t)$ , and the phase  $\varphi(\mathbf{r},t)$  are given by Eqs. (6a)–(6c).

For the illustrative purposes, we can choose these free parameters in the form

$$c_\sigma(t) = a_\sigma(t) = \text{dn}(t, k_\sigma), \quad \rho_0 = 1, \quad \gamma(t) = \text{sn}(t, k) \text{cn}(t, k) \quad (13)$$

(where dn, sn, and cn stand for the respective Jacobi elliptic functions, and  $k_\sigma, k$  are their moduli) and  $\omega(t)=0$ . Figure 1 depicts the profiles of nonlinearity  $g(t)$  given by Eq. (7b), the coefficients of second degree terms of the linear potential  $v(\mathbf{r},t)$  given by Eq. (8), and the gain or loss term  $\gamma(t)$  vs time for the chosen parameters given by Eq. (13). The evolution of intensity distribution of the 3D field (12) is shown in Fig. 2. We can see that the simple Lorentzian function of the (1 + 1)-dimensional case is transformed into a significantly more complicated evolution along the  $t$  axis. The solution is localized in space and keeps the localization infinitely in time, which differs from the usual rogue wave solutions (see [23]).

On the other hand, if we choose the free parameters in the form

$$\begin{aligned} c_x(t) &= a_x(t) = 1 + c_0 \sin(t), \\ c_y(t) &= a_y(t) = 1.2 + c_0 \cos(t), \\ c_z(t) &= a_z(t) = 0.8 + c_0 \sin(t), \quad c_0 = 0.01, \end{aligned} \quad (14)$$

and  $\rho_0$ ,  $\omega(t)$ , and  $\gamma(t)$  are same as the ones given by Eq. (13), then the evolution of intensity distribution of the 3D rogue wave solutions (12) will be changed. Figure 3 displays the profiles of nonlinearity  $g(t)$  given by Eq. (7b) and the coefficients of second degree terms of the linear potential  $v(\mathbf{r},t)$  given by Eq. (8) vs time for the chosen parameters given by Eq. (14). For this case, the 3D rogue wave solution (12) is shown in Fig. 4. The solution is localized both in time and in space, thus revealing the usual “rogue wave” features. It is worth emphasizing here that although the “generating” function  $c(t)$  was chosen as a monochromatic function, the respective change in the nonlinearity  $g(t)$  required for the existence of the exact solution is periodic, but depending on various frequencies. This is natural reflection of the fact that we are dealing with a nonstationary solution of the nonlinear problem, characterized by the generation of multiple frequencies.

Generally speaking, we have large degree of freedom in choosing the coefficients of transformation. As a result, we can describe infinitely large class of solutions of the three-

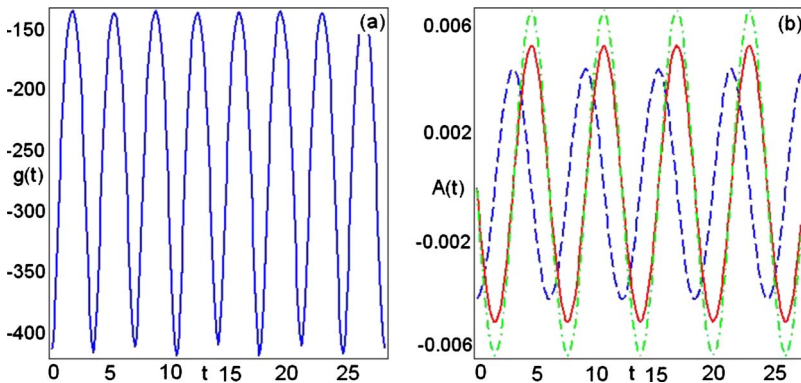


FIG. 3. (Color online) Profiles of (a) nonlinearity  $g(t)$  given by Eq. (7b) and (b) the coefficients  $A_x(t)$  (solid line),  $A_y(t)$  (dashed line), and  $A_z(t)$  (dashed-dotted line) of second degree term of the linear potential  $v(\mathbf{r},t)$  given by Eq. (8) vs time for the parameters are given by Eq. (14).



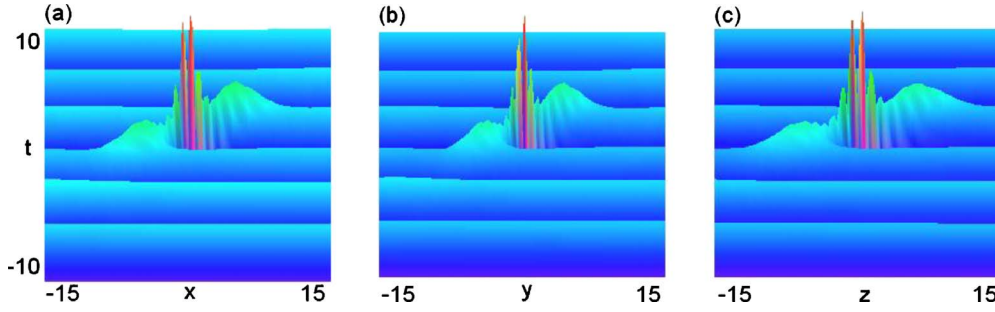


FIG. 4. (Color online) Color coded plot of wave intensity (a)  $|\Psi_1|^2(x,0,0,t)$  with  $\max_{\{x,0,0,t\}}|\Psi_1|^2=0.027$ , (b)  $|\Psi_1|^2(0,y,0,t)$  with  $\max_{\{0,y,0,t\}}|\Psi_1|^2=0.03$ , and (c)  $|\Psi_1|^2(0,0,z,t)$  with  $\max_{\{0,0,z,t\}}|\Psi_1|^2=0.029$  defined by solution (12) for the parameters given by Eq. (14).

dimensional NLS equation with every exact solution of the one-dimensional NLS equation. Additional possibility of choosing the solution of the latter one increases tremendously the variety of solutions that we can obtain.

When a higher-order rational solution of the NLS equation (2) (see [23,24]) is applied to transformation (4), we obtain the second-order nonstationary rogue wave solutions of Eq. (1) in the form

$$\Psi_2(\mathbf{r}, t) = \rho_0 \sqrt{|c_x(t)c_y(t)c_z(t)|} \exp \left[ \int_0^t \gamma(s) ds \right] \times \left[ 1 + \frac{P(\eta, \tau) - i\tau(t)Q(\eta, \tau)}{H(\eta, \tau)} \right] e^{i[\varphi(\mathbf{r}, t) + \tau(t)]}, \tag{15}$$

where the functions  $P(\eta, \tau)$ ,  $Q(\eta, \tau)$ , and  $H(\eta, \tau)$  are given by [24]

$$P(\eta, \tau) = -\frac{1}{2}\eta^4 - 6\eta^2\tau^2 - 10\tau^4 - \frac{3}{2}\eta^2 - 9\tau^2 + \frac{3}{8},$$

$$Q(\eta, \tau) = \eta^4 + 4\eta^2\tau^2 + 4\tau^4 - 3\eta^2 + 2\tau^2 - \frac{15}{4},$$

$$H(\eta, \tau) = \frac{1}{12}\eta^6 + \frac{1}{2}\eta^4\tau^2 + \eta^2\tau^4 + \frac{2}{3}\tau^6 + \frac{1}{8}\eta^4 + \frac{9}{2}\tau^4 - \frac{3}{2}\eta^2\tau^2 + \frac{9}{16}\eta^2 + \frac{33}{8}\tau^2 + \frac{3}{32}. \tag{16}$$

The variables  $\eta(\mathbf{r}, t)$ ,  $\tau(t)$ , and the phase  $\varphi(\mathbf{r}, t)$  here are given by Eqs. (6a)–(6c).

As in the previous cases, we choose the parameters given by Eqs. (13) and (14) except for  $a_\sigma(t)=0$ . The intensity distributions of the second-order rogue wave solutions (15) are depicted in Figs. 5 and 6. Clearly, the field evolution in this case is more complicated. In one case, shown in Fig. 5, the solution is localized in all three dimensions in space. In the other case, shown in Fig. 6 the solution is localized both in space and in time, thus displaying the basic feature of a rogue wave that “appears from nowhere and disappears without a trace.”

It follows from the above-mentioned two cases for the parameters that the parameters  $c_\sigma(t)$ ,  $a_\sigma(t)$ , and  $\gamma(t)$  can be used to control the wave propagations related to rogue waves, which may raise the possibility of relative experiments and potential applications in nonlinear optics and BECs. Similarly we can also obtain three-dimensional higher-order time-dependent rogue wave solutions of Eq. (1) in terms of transformation (4) and higher-order rogue wave solutions of the NLS equation (2), which are omitted here.

As always happen with the nonlinear Schrödinger equation in two and three dimensions, their localized solutions

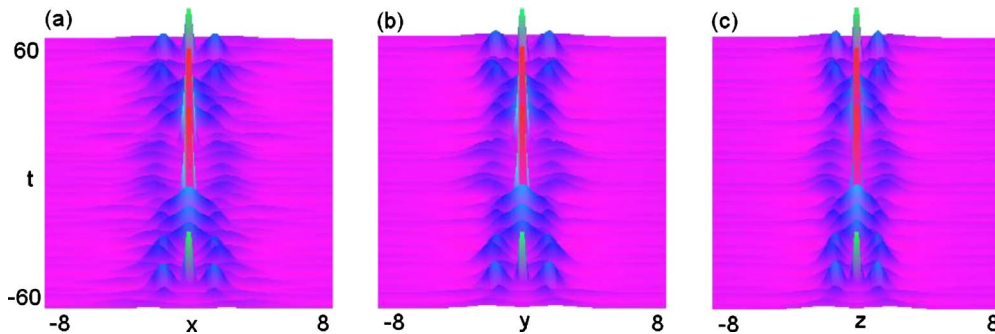


FIG. 5. (Color online) Color coded wave intensity (a)  $|\Psi_2|^2(x,0,0,t)$  with  $\max_{\{x,0,0,t\}}|\Psi_2|^2=0.135$ , (b)  $|\Psi_2|^2(0,y,0,t)$  with  $\max_{\{0,y,0,t\}}|\Psi_2|^2=0.13$ , and (c)  $|\Psi_2|^2(0,0,z,t)$  with  $\max_{\{0,0,z,t\}}|\Psi_2|^2=0.125$  given by solution (15) for  $a_\sigma(t)=0$  and other parameters given by Eq. (13) with  $k_x=0.9$ ,  $k_y=0.6$ ,  $k_z=0.1$ , and  $k=0.6$ .

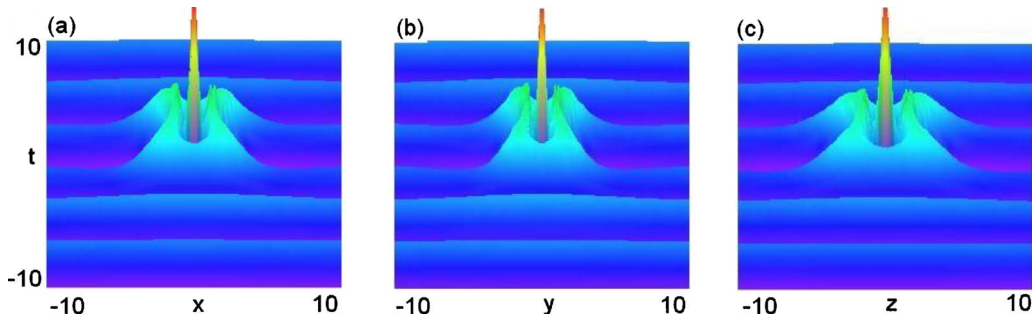


FIG. 6. (Color online) Color coded wave intensity (a)  $|\Psi_2|^2(x,0,0,t)$  with  $\max_{\{x,0,0,t\}}|\Psi_2|^2=0.038$ , (b)  $|\Psi_2|^2(0,y,0,t)$  with  $\max_{\{0,y,0,t\}}|\Psi_2|^2=0.036$ , and (c)  $|\Psi_2|^2(0,0,z,t)$  with  $\max_{\{0,0,z,t\}}|\Psi_2|^2=0.038$  given by solution (15) for  $a_\sigma(t)=0$  and other parameters given by Eq. (14).

may collapse. The stability of the solutions presented in our work is still an open question. This question deserves separate studies, as it is a task that is far from being trivial. We leave these studies to later publications.

## V. CONCLUSIONS

In conclusion, we have presented similarity reductions of the (3+1)-dimensional inhomogeneous nonlinear Schrödinger equation with variable coefficients to the (1+1)-dimensional one with constant coefficients. This transformation allows us to relate certain class of localized solutions of the (3+1)-dimensional case to the variety of solutions of integrable NLS equation of the (1+1)-dimensional case. As an example, we illustrated our

technique by two lowest-order rational solutions of the NLSE. These are transformed into rogue wave solutions localized in 3D space that have complicated evolution in time. The technique may also be extended to other NLS-type equations to exhibit their rogue wave solutions.

## ACKNOWLEDGMENTS

Z.Y. gratefully acknowledges the support of the NSFC Contract No. 60821002/F02. The research of V.V.K. was partially supported by Grant No. PIF-GA-2009-236099 (NOMATOS) within the 7th European Community Framework Programme. N.A. gratefully acknowledges the support of the Australian Research Council (Discovery Project No. DP0985394).

- 
- [1] G. W. Bluman and S. Kumei, *Symmetries and Differential Equations* (Springer-Verlag, New York, 1989); P. J. Olver, *Application of Lie Groups to Differential Equations*, 2nd ed. (Springer-Verlag, New York, 1993); G. W. Bluman, A. Cheviakov, and S. Anco, *Applications of Symmetry Methods to Partial Differential Equations* (Springer, New York, 2009); G. W. Bluman and Z. Y. Yan, *Eur. J. Appl. Math.* **16**, 239 (2005).
- [2] M. Ablowitz and H. Segur, *Solitons and the Inverse Scattering Transform* (SIAM, Philadelphia, 1981).
- [3] R. Y. Chiao, E. Garmair, and C. H. Townes, *Phys. Rev. Lett.* **13**, 479 (1964).
- [4] V. N. Vlasov, I. A. Petrishev, and V. I. Talanov, *Izv. Vyssh. Uchebn. Zaved., Radiofiz.* **14**, 1353 (1971).
- [5] L. Berge, *Phys. Rep.* **303**, 259 (1998).
- [6] C. A. Akhmanov and R. V. Khokhlov, *Problems of Nonlinear Optics: Electromagnetic Waves in Nonlinear Dispersive Media* (VINITI, Moscow, 1964).
- [7] L. Gagnon, *J. Opt. Soc. Am. B* **7**, 1098 (1990).
- [8] Y. S. Kivshar and G. P. Agrawal, *Optical Solitons: From Fibers to Photonic Crystals* (Academic, New York, 2003); B. A. Malomed, D. Mihalache, F. Wise, and L. Torner, *J. Opt. B: Quantum Semiclassical Opt.* **7**, R53 (2005).
- [9] L. Pitaevskii and S. Stringari, *Bose-Einstein Condensation* (Oxford University Press, Oxford, 2003); R. Carretero-González, D. J. Frantzeskakis, and P. G. Kevrekidis, *Nonlinearity* **21**, R139 (2008); F. Dalfovo, S. Giorgini, L. P. Pitaevskii, and S. Stringari, *Rev. Mod. Phys.* **71**, 463 (1999); A. J. Leggett, *ibid.* **73**, 307 (2001).
- [10] Z. Y. Yan and V. V. Konotop, *Phys. Rev. E* **80**, 036607 (2009).
- [11] Z. Y. Yan and C. Hang, *Phys. Rev. A* **80**, 063626 (2009).
- [12] A. R. Osborne, *Nonlinear Ocean Waves* (Academic, New York, 2009).
- [13] A. Montina, U. Bortolozzo, S. Residori, and F. T. Arecchi, *Phys. Rev. Lett.* **103**, 173901 (2009).
- [14] M. Shats, H. Punzmann, and H. Xia, *Phys. Rev. Lett.* **104**, 104503 (2010).
- [15] D. R. Solli, C. Ropers, P. Koonath, and B. Jalali, *Nature (London)* **450**, 1054 (2007); D. R. Solli, C. Ropers, and B. Jalali, *Phys. Rev. Lett.* **101**, 233902 (2008).
- [16] D.-I. Yeom and B. Eggleton, *Nature (London)* **450**, 953 (2007).
- [17] Yu. V. Bludov, V. V. Konotop, and N. Akhmediev, *Opt. Lett.* **34**, 3015 (2009).
- [18] Z. Y. Yan, *Phys. Lett. A* **374**, 672 (2010).
- [19] Yu. V. Bludov, V. V. Konotop, and N. Akhmediev, *Phys. Rev. A* **80**, 033610 (2009).
- [20] L. Stenflo and M. Marklund, *J. Plasma Phys.* **76**, 293 (2010).
- [21] Z. Y. Yan, e-print [arXiv:0911.4259](https://arxiv.org/abs/0911.4259).
- [22] J. Belmonte-Beitia, V. M. Pérez-García, V. Vekslerchik, and V. V. Konotop, *Phys. Rev. Lett.* **100**, 164102 (2008).

- [23] N. Akhmediev, A. Ankiewicz, and J. M. Soto-Crespo, *Phys. Lett. A* **373**, 2137 (2009).
- [24] N. Akhmediev, A. Ankiewicz, and M. Taki, *Phys. Lett. A* **373**, 675 (2009); see also N. Akhmediev, V. M. Eleonskii, and N. E. Kulagin, *Sov. Phys. JETP* **89**, 1542 (1985).
- [25] N. Akhmediev, A. Ankiewicz, and J. M. Soto-Crespo, *Phys. Rev. E* **80**, 026601 (2009).
- [26] A. Ankiewicz, P. A. Clarkson, and N. Akhmediev, *J. Phys. A* **43**, 122002 (2010).